DETECTION OF INLAND WATER BODIES WITH HIGH TEMPORAL RESOLUTION – ASSESSING DYNAMIC THRESHOLD APPROACHES

Igor Klein, Ursula Gessner*, Andreas Dietz*, Patrick Leinenkugel*, Stefan Dech*, Claudia Kuenzer**

*German Aerospace Center (DLR), German Remote Sensing Data Center (DFD)

ABSTRACT

Information on the spatio-temporal dynamics of inland water bodies is of high value for many applications, for example in the context of water and land management or for ecosystem service assessments. In this study, different approaches to delineate inland water bodies from MODIS 250 m time series were compared. Here, the performance of different input bands and indices, of trainings pixel selection methods, and of dynamic threshold definition approaches were assessed with the goal to find an optimized approach applicable for global inland water body detection based on moderate spatial and high temporal resolution MODIS data. The results of the tested approaches were cross validated with high resolution Landsat-8 classifications. The results show amongst others that a combination of near infrared band (NIR) and difference index (NIR – red band) performed best for most of the globally distributed test regions and that single band approaches revealed higher commission errors.

***Index Terms*— inland water bodies dynamics, time series analysis, MODIS**

1. INTRODUCTION

The distribution of inland waters bodies and their seasonal variability is a key factor for ecosystems, and human livelihoods. Knowledge on inland water distribution and variability is required for water and land management, and forms an important information basis for decision makers and science, especially in the field of regional and global environmental research. There are many valuable global water datasets with high precision and accuracy. For example the latest MODIS global 250 m water mask [1], the Global Lakes and Wetlands Database, GLWD [2], the global map of open permanent water bodies [3] or the Global Water Bodies (GLOWABO) map with 30m spatial resolution [4]. However, these products mirror only a static situation or a temporal snap shot [5]. Recently many studies are exploiting the availability of time series covering long periods to reconstruct the dynamics of inland water bodies. These studies use temporal composites and cover only certain regions e.g. [6]–[9]. Our goal is to develop a methodology which allows a reconstruction of global inland water body dynamics by fully exploiting the daily resolution of MODIS. In this paper we assessed selected threshold definition strategies in order to find an optimal method for detecting inland water bodies globally with diurnal temporal resolution. Landsat images were used for validation across the globe.

2. DATA AND MATERIALS

Input data for dynamic surface water classification are the MODIS level-2 reflectances MOD09GQ/MYD09GQ, as well as the level-3 snow cover products MOD10A1/MYD10A1. There are three main reasons for using MODIS data which are a particularly useful resource for continental and global environmental assessments. First, the data is available since February 2000 and has a high temporal resolution of one day and moderate spatial resolution of 250m for the near infra-red band (841-876 nm) and the red band (620-670 nm). Secondly, since July 2002 equivalent data are available from the Terra and Aqua satellites, which allow detecting one area twice a day. Thirdly, the MODIS gridded level-2 products MOD09GQ/MYD09GQ (4800*4800 pixels per tile in Sinusoidal projection) are free of charge and easily accessible. They are provided as calibrated spectral radiance values estimating surface spectral reflectance at ground level, corrected for atmospheric influence [10]. The thematic level-3 MOD10A1/MYD10A1 product provides information on daily snow cover, lake ice and cloud cover and also includes a static ocean mask, inland water mask.

For cross validation purpose we decided to use freely available Landsat-8 data with a spatial resolution of 30 m. In total 152 images were analyzed for different eco-regions covering different environmental and hydrological conditions, distributed all over the globe. The images comprise stable water bodies, water bodies which expand and shrink over the year as well as areas with singular flood events.

Furthermore, we used the latest static water mask product MOD44W introduced by [1] to identify possible training areas as well a digital elevation model (DEM) from [12] to identify steep slopes and topographic shadows.

3. METHODOLOGY

3.1. Pre-processing

We acquired a range of different earth observation datasets with different geographical projections and spatial resolutions. To allow an automatic processing we introduced a pre-processing step which harmonizes all the input data. All input and ancillary data were resampled with nearest neighbor technique and re-projected to suit the MOD09G/MYD09GQ data with spatial resolution of 250 m in sinusoidal projection. In this way a simple and fast pixel to pixel analysis is enabled.

3.2. Performance Assessment

The aim of this study is twofold. First, to assess the performance of training pixels extracted from the MOD44W static water mask, and second, to compare different dynamic threshold settings for water delineation. We applied the tests on three different input feature sets: on single band sets of near infrared (NIR), and difference index (Dif_{Index}) and on the combination of NIR and Dif_{Index}. The NIR single band methodology has been used in many studies with reasonable results due to the unique characteristic of water to absorb the electromagnetic radiance in this range, which results in low reflectance in this spectral region [13], [14]. The Dif_{Index} was proposed to be well suited index and most useful to delineate between inland water and land [15]. However, the NIR band and The Dif_{Index} might be unsuitable for global usage on a diurnal basis for various reasons (cloud shadow, relief shadow, snow and not identified clouds). Therefore, we also test the combination of NIR band and Dif_{Index}.

As we use static water mask for training pixel selection it is crucial to excluded all regions which are covered by clouds or lake ice at the moment of observation. For this purpose the MOD10A1/MYD10A1 products were used. However, our analyses showed that not all cloud covered and lake ice covered pixels are labeled through this procedure. Furthermore, we exclude all pixels which are labeled as ocean as these pixels are not suitable to classify inland water bodies and especially temporally flooded areas. Additionally, there is one main factor to be considered: the MOD44W is a static water mask which was developed based on multiple datasets covering a time span of about six years [1]. Therefore, particularly for dynamic water bodies, not all static water pixels might be indeed water at the date of a MODIS observation. To illustrate this issue, one might imagine the size of the well-known Aral Sea between 2003 and 2009 and the fact that the lake's eastern lobe of the southern part was dried out by 2014 [6]. Using all water labeled pixels for training would include also the desiccated areas and thus contaminate the threshold considerably.

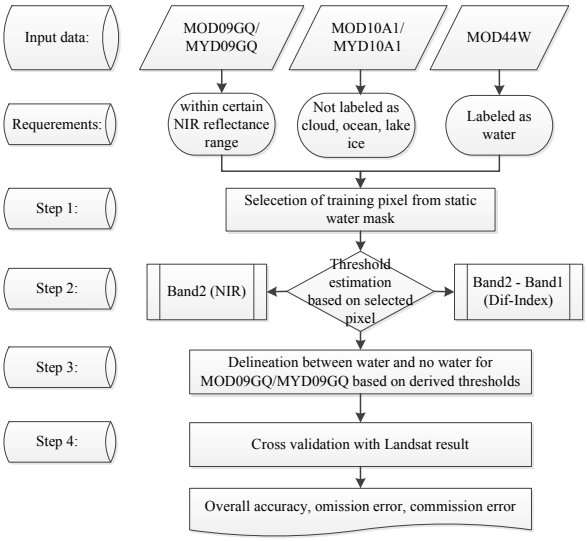

Figure 1: Workflow

Therefore, we tested how to best restrict the selection of valid training pixels from the static water mask to only those water labeled pixels in MOD44W which are not covered by cloud, ocean, or lake ice (according to MOD10A1/MYD10A1). In this context, we examined the applicability of an additional criterion for training pixel candidates in the form of six spectral reflectance ranges in the NIR: 0-15%, 0-17,5%, 0-20%, 0-22,5%, 0-25%, 0-100%.

With regard to the water mask classification we tested different percentiles (50%, 65%, 70%, 75%, 80%, 85%, 90%, 95%, 99%) to be used as dynamic thresholds. The water classification was performed for NIR, Dif_{Index}, and the combination of both after the workflow illustrated in Figure 1.

3.3. Classification of Landsat images

Many remote sensing studies working with moderate resolution data are using higher spatial resolution data to validate their results [1], [16], [17]. We decided to utilize Landsat-8 data for the validation of our results. We applied a semi-automatic classification based on the Normalized Difference Water Index (NDWI, after [18]), Normalized Vegetation Index (NDVI) and several other band conditions to detect water. Furthermore, cloud and cloud shadows were classified by using the function of mask (FMASK) approach [19]. Each image was manually examined by an image interpreter for possible errors. In case of over- or

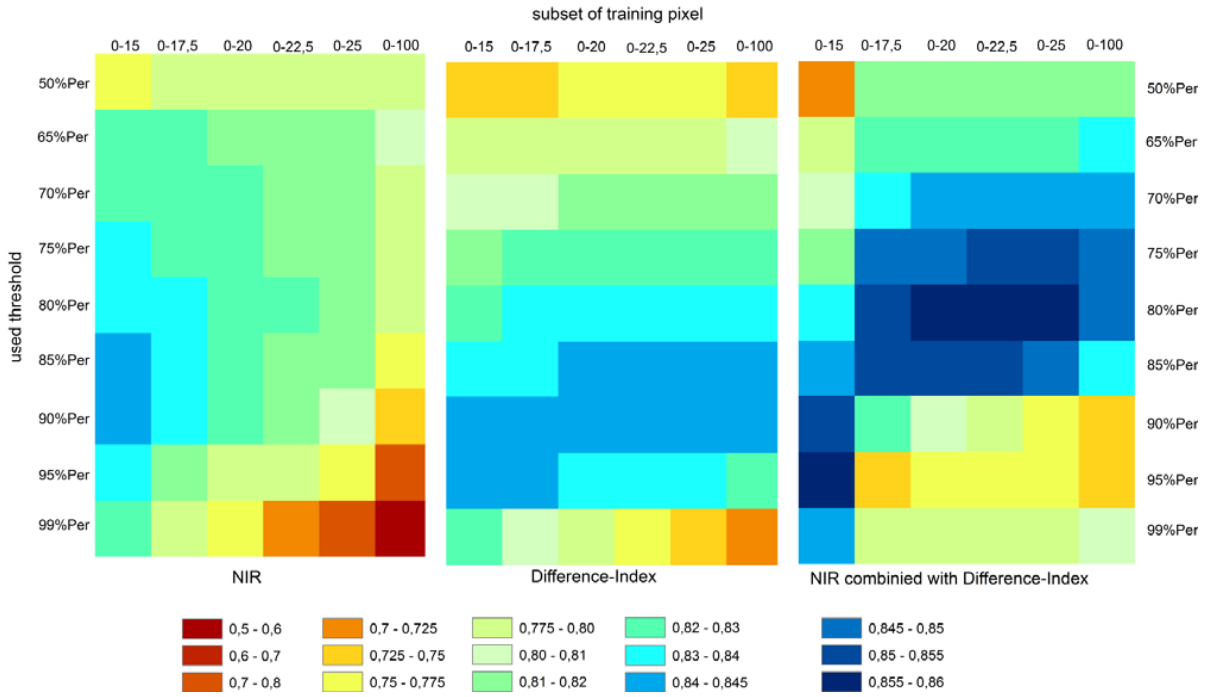

Figure 2: Matrix of calculated overall accuracies for the tested approaches for boreal and sub-polar regions

underestimation the image underwent manual improvements to fulfil the required accuracy for a validation dataset. In this way we achieved 152 Landsat classifications with high confidence of correctness.

3.4. Validation

The results of all classification approach variants as described in section 3.2 were validated with the Landsat classification to evaluate the overall accuracy, omission and commission errors. A set of 10.000 land and 10.000 water pixels from each of the 152 Landsat classifications was selected randomly.

4. RESULTS AND DISCUSSION

The comparative study provides three main outcomes. First, the performance of training pixels can be clearly improved by excluding outlier pixels with extraordinarily high NIR reflectances from the sample dataset, in addition to masking with MOD10A1/MYD10A1. Reasons are on the one hand the cloud mask used in MOD10A1/MYD10A1 which features over- and underestimations. Remaining cloud- and ice-affected pixels in the training dataset increase the thresholds which lead to overestimation of surface water and higher commission errors. On the other hand desiccated areas (labeled as water in MOD44W) also increase the thresholds and thus can lead to overestimations of water.

As an example, Figure 2 illustrates the results considering all Landsat reference classifications in boreal and sub-polar regions. It is clearly visible that masking potential training areas by MOD10A1/MYD10A1without an additional NIR threshold (compare Figure 2, subset training pixel: 0-100% on the x-axis) provides the worst results regarding only NIR single band approach. In this region the effect is most probable due to lake ice and clouds rather than desiccated areas. The effect is less dominant for Dif_{Index} and the combination. The evaluation of different input feature sets showed that in most cases the combination of NIR band and Dif_{Index} achieved the best results. Depending on the climatic and surrounding land surface conditions improvements are more or less pronounced. For example, in presence of clouds and cloud shadows the single band NIR approach featured higher commission errors than Dif_{Index} or the combination. In contrast, when using only the Dif_{Index}, overestimations for bright land covers (snow cover, salt pans) occurred. Finally, the best definition of the dynamic threshold settings revealed that for the combination of Dif_{Index} and NIR thresholds of 75%, 80%, 85% percentiles were most successful.

5. CONCLUSION

The aim of this study was to assess approaches for water delineation on daily MODIS data in a range of different environmental conditions. The results proof that a combination of NIR band and Dif_{Index} can be used for water classification on global scale successfully. A strict definition of training pixels excluding high samples with extraordinarily high NIR reflectance values improved the accuracy and diminished overestimation of water. The outcomes of this feasibility study will be exploited for further global application and derivation of water bodies and their spatial variability.

6. REFERENCES

[1] M. L. Carroll, J. R. Townshend, C. M. DiMiceli, P. Noojipady, and R. a. Sohlberg, "A new global raster water mask at 250 m resolution," *Int. J. Digit. Earth*, vol. 2, no. 4, pp. 291–308, Dec. 2009.

[2] B. Lehner and P. Döll, "Development and validation of a global database of lakes, reservoirs and wetlands," *J. Hydrol.*, vol. 296, no. 1–4, pp. 1–22, Aug. 2004.

[3] ESA Climate Change Initiative, "Global Water Bodies," 2014. [Online]. Available: http://www.esa-landcover-cci.org/?q=node/162.

[4] C. Verpoorter, T. Kutser, D. A. Seekell, and L. J. Tranvik, "A global inventory of lakes based on high-resolution satellite imagery," pp. 1–7, 2014.

[5] B. Fichtelmann and E. Borg, "A New Self-Learning Algorithm for Dynamic Classification of Water Bodies," in *Computational Science an Its Applications - ICCSA 2012, Part III*, 2012, pp. 457–470.

[6] I. Klein, A. J. Dietz, U. Gessner, A. Galayeva, A. Myrzakhmetov, and C. Kuenzer, "Evaluation of seasonal water body extents in Central Asia over the past 27 years derived from medium-resolution remote sensing data," *Int. J. Appl. Earth Obs. Geoinf.*, vol. 26, pp. 335–349, Feb. 2014.

[7] J.-F. Pekel, C. Vancutsem, L. Bastin, M. Clerici, E. Vanbogaert, E. Bartholomé, and P. Defourny, "A near real-time water surface detection method based on HSV transformation of MODIS multi-spectral time series data," *Remote Sens. Environ.*, vol. 140, pp. 704–716, Jan. 2014.

[8] E. M. Haas, E. Bartholomé, and B. Combal, "Time series analysis of optical remote sensing data for the mapping of temporary surface water bodies in sub-Saharan western Africa," *J. Hydrol.*, vol. 370, no. 1–4, pp. 52–63, May 2009.

[9] L. Feng, C. Hu, X. Chen, X. Cai, L. Tian, and W. Gan, "Assessment of inundation changes of Poyang Lake using MODIS observations between 2000 and 2010," *Remote Sens. Environ.*, vol. 121, pp. 80–92, Jun. 2012.

[10] "Land Processes Distributed Active Archive Center," 2015. [Online]. Available: https://lpdaac.usgs.gov/.

[11] D. K. Hall and G. A. Riggs, "Accuracy assessment of the MODIS snow products †," vol. 1547, pp. 1534–1547, 2007.

[12] "Consortium for Spatial Information (CGIAR-CSI)," 2009. [Online]. Available: http://www.cgiar-csi.org/.

[13] J. Ryu, J. Won, and K. D. Min, "Waterline extraction from Landsat TM data in a tidal flat A case study in Gomso Bay , Korea," vol. 83, pp. 442–456, 2002.

[14] L. C. Smith, "SATELLITE REMOTE SENSING OF RIVER INUNDATION AREA , STAGE , AND DISCHARGE : A REVIEW," vol. 11, no. April 1996, pp. 1427–1439, 1997.

[15] D. Sun, Y. Yu, and M. D. Goldberg, "Deriving Water Fraction and Flood Maps From MODIS Images Using a Decision Tree Approach," *IEEE J. Sel. Top. Appl. Earth Obs. Remote Sens.*, vol. 4, no. 4, pp. 814–825, Dec. 2011.

[16] A. J. Dietz, C. Kuenzer, and C. Conrad, "Snow-cover variability in central Asia between 2000 and 2011 derived from improved MODIS daily snow-cover products," *Int. J. Remote Sens.*, vol. 34, no. 11, pp. 3879–3902, Jun. 2013.

[17] W. Li, Z. Du, F. Ling, D. Zhou, H. Wang, Y. Gui, B. Sun, and X. Zhang, "A Comparison of Land Surface Water Mapping Using the Normalized Difference Water Index from TM, ETM+ and ALI," *Remote Sens.*, vol. 5, no. 11, pp. 5530–5549, Oct. 2013.

[18] B. Gao, "NDWI A Normalized Difference Water Index for Remote Sensing of Vegetation Liquid Water From Space," vol. 266, no. April 1995, pp. 257–266, 1996.

[19] Z. Zhu and C. E. Woodcock, "Object-based cloud and cloud shadow detection in Landsat imagery," *Remote Sens. Environ.*, vol. 118, pp. 83–94, 2012.